

Electrosynthesis And Studies on $Zn_{1-x}Hg_xTe$ Thin Films

*T. Mahalingam^{1,5}, A. Kathalingam², S. Velumani³, Soonil Lee⁴, Hosun Moon⁵ and Yong Deak Kim⁵

¹Department of Physics, Alagappa University, Karaikudi – 630 003, India

²Department of Physics, Periyar Maniammai college of Technology for women, Vallam, Thanjavur-613403, India

³Departamento de Fisica, ITESM - Campus Monterrey, Nuevo Leon, C.P.64849, Mexico

⁴Department of Molecular Science and Technology, Ajou University, Suwon 442-749, Korea

⁵Department of Electrical and Computer Engineering, College of Information Technology, Ajou University, Suwon 443-749, Korea

Received: August 15, 2005, Accepted: January 8, 2006

Abstract: The electrodeposition and characterization of $Zn_{1-x}Hg_xTe$ (ZMT) thin films is reported in this work. The films were deposited onto SnO_2 coated glass substrates from an aqueous solution bath of $ZnSO_4$, $HgCl_2$ and TeO_2 at bath temperatures between 30 °C and 80 °C. Well adherent $Zn_{1-x}Hg_xTe$ films with compositions varying between $x = 0$ to $x = 0.4$ were obtained. The effect of growth parameters such as deposition potential, concentration of electrolyte bath, pH and temperature on the properties of the film was studied. X-ray diffraction technique was used to determine composition, crystalline structure and grain size of the films. The films exhibited zinc blend structure with predominant (111) orientation. Optical and electrical studies were also studied and the results are discussed.

Keywords: Electrodeposition, Thin Films, Zinc Mercury Telluride, and Ternary alloy

1. INTRODUCTION

The ever increasing technological needs for micro and optoelectronic devices, such as light emitting diodes (LEDs) and photodetectors (PDs), operating in the spectral regions from visible to far-infrared continues to attract much of the current research activities on the thin films of different wide-gap and narrow-band semiconductor heterostructures and compounds [1-3]. Among II-VI based heterostructures with potential applications to the realization of efficient PDs, many efforts have been focused on heterostructures based on popularly known ternary solid solution $Cd_xHg_{1-x}Te$ ($0 < x < 1$) thin films as well as bulk materials [4-6]. $CdTe$, $HgCdTe$ and other compounds of II^AVI^B group are very promising materials for use in optoelectronic and high-temperature electronic devices. Ternary alloys of II-VI compounds are potential candidates for the detection of electromagnetic radiation. Zinc mercury telluride, a solid solution has a wide range of band gap tunability between 0 eV and 2.25 eV. It offers potential advantages over Cd based $HgCdTe$, $HgCdSe$ due to its high stability [7]. Recently, ternary compounds have received much attention in the

field of solar cells owing to their interesting properties of band gap and lattice constant modulation by composition variation [8,9]. To date, a number of growth techniques, in particular, molecular-beam epitaxy (MBE) and liquid-phase epitaxy (LPE) have been employed to grow different structures based on II-VI materials [10-12], but the work on $ZnHgTe$ reported in the literature is scarce and we are interested to study $Zn_{1-x}Hg_xTe$ thin films prepared by electrodeposition. Electrodeposition offers a low - cost, scalable technique for the fabrication of thin films. The influence of various growth parameters on the deposition of crystalline stoichiometric $Zn_{1-x}Hg_xTe$ films are studied and reported in this paper.

2. EXPERIMENTAL DETAILS

All the chemicals used in this work were of analytical reagent grade (99 % purity, E-Merck). The zinc mercury telluride films were deposited onto fluorine doped SnO_2 coated conducting glass plates (15 ohms/square) by co - deposition of zinc, mercury and tellurium ions. The electrolyte bath was consisted of an aqueous solution of $ZnSO_4$ (10 – 30 mM), $HgCl_2$ (0.1 – 1.5 mM) and TeO_2 (1 – 5 mM). As the solubility of TeO_2 is less at high pH, it requires

*To whom correspondence should be addressed: Email: tmaha51@yahoo.com

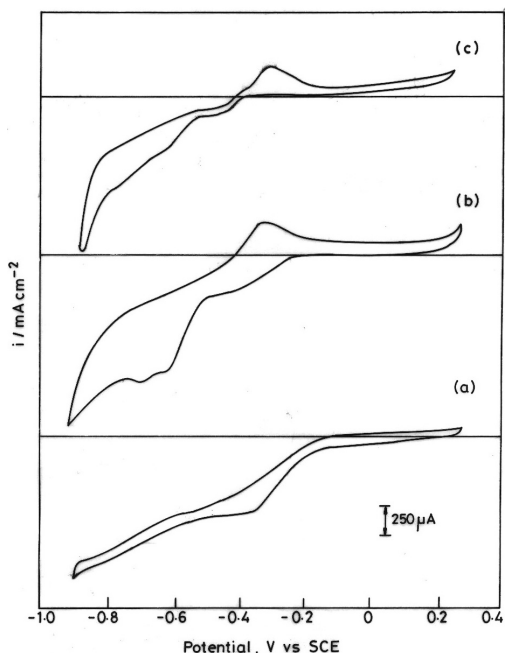


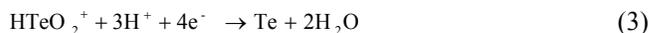
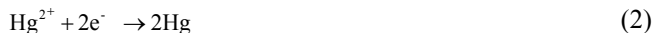
Figure 1. Cyclic voltammograms on tin oxide coated glass electrode: Curve (a): TeO_2 ; Curve (b): $\text{TeO}_2 + \text{ZnSO}_4$; Curve (c): $\text{TeO}_2 + \text{HgCl}_2 + \text{ZnSO}_4$

several hours for its dissolution. To avoid this problem, an acidic solution was prepared by dissolving TeO_2 in H_2SO_4 and then it was heated for 15 minutes to prepare stock solution. The conducting tin oxide coated glasses of approximately 1 cm^2 area were cleaned before deposition with detergent, dried and degreased with acetone and distilled water. The depositions were carried out cathodically using a potentiostat (EG & G, Princeton Applied Research, USA, Model 362) with standard three-electrode arrangement such as working electrode (substrate), counter electrode (graphite) and reference electrode (saturated calomel electrode-SCE). Series of films were deposited at different potentials ranging from -0.6 V to -1.2 V versus SCE for various bath concentrations and temperatures. The pH of the electrolyte was kept between 2 and 4. After film formation, the samples were rinsed with distilled water, dried and stored in a desiccator for further studies. The film thickness was measured using multiple beam interferometer and found to be in the range between 150 and 400 nm. Deposited films were analyzed using an x-ray diffractometer (Philips Model PW1710) using CuK_α radiation with $\lambda = 0.15418 \text{ nm}$. Surface morphological and compositional analysis were carried out using a scanning electron microscope and energy dispersive X-ray analysis set up (EDAX) attached with SEM, respectively (Philips, Model XL 30). Optical measurements were carried out using a JASCO V-570 spectrophotometer.

3. RESULTS AND DISCUSSION

The electrodeposition of II-VI ternary compounds is more complex as they involve different constituents of varying deposition potentials. The main chemical reactions involved in the electrode-

position of $\text{Zn}_{1-x}\text{Hg}_x\text{Te}$ are as follows:



$\text{Zn}_{1-x}\text{Hg}_x\text{Te}$ films were found to be adhered well with the substrates. The composition of the films was found to vary from $x = 0$ to $x = 0.4$ for films deposited under optimized conditions. The optimum deposition conditions for the deposition of $\text{Zn}_{1-x}\text{Hg}_x\text{Te}$ films are identified as: Deposition potential -0.85 V vs SCE, Solution pH: 3.0, Bath temperature: 80°C and Current density: 1.5 mA cm^{-2} .

3.1. Cyclic voltammetric study

Voltammograms of plating baths of different compositions give further information on the possible range of deposition potentials. Fig.1 (a) shows a scan for a tin oxide coated glass electrode in a solution containing TeO_2 (4 mM) at $\text{pH } 3.0 \pm 0.1$. Upon scanning towards more negative potentials, a reduction wave for HTeO_2^+ to Te at -0.4 V versus SCE and a dark gray film of Te on the electrode were observed. Addition of ZnSO_4 (10 mM) resulted in an additional reduction wave at -0.6 V versus SCE (Fig.1.b) and the reduction wave of HTeO_2^+ about -0.4 V together with a decrease in its plateau current. This indicates a radical change in the reaction mechanism; the decrease of current around -0.4 V in the presence of large amount of Zn^{2+} can be explained by its competition with Te precursors for adsorption sites. The anodic wave at -0.6 V vs SCE can be ascribed to the formation of ZnTe . In curve (c), the reduction of the three precursors is shown. The wave centered at -0.6 V is ascribed the formation of the compound $\text{Zn}_{1-x}\text{Hg}_x\text{Te}$. Beyond -0.9 V , the current increase rapidly indicating the hydrogen evolution and it has been found that the deposits obtained at potentials below -0.9 V are not adhered to the substrates and found to be peeled out due to hydrogen evolution. Based on the above results, a deposition potential range between -0.6 and -1.0 V was selected to deposit $\text{Zn}_{1-x}\text{Hg}_x\text{Te}$ films in the present work.

3.2. Effect of pH and deposition potential

Deposition of $\text{Zn}_{1-x}\text{Hg}_x\text{Te}$ films was carried out using an electrolyte with the pH value varying between 2 and 4. The pH of the electrolyte was found to have a strong influence on the composition of the films. For pH below 2.5, excessive amount of pure Te was deposited while at pH greater than 4, insufficient Te could be dissolved in the electrolyte to produce stoichiometric films. At $\text{pH} < 2$, deposition was also hindered due to hydrogen evolution and adherence of deposited films with the substrates was poor. Films deposited at pH 3.0 have yielded significant results. Therefore, the pH of the solution in the present work was kept at 3.0. $\text{Zn}_{1-x}\text{Hg}_x\text{Te}$ films were deposited at different potentials ranging from -0.6 V to -1.0 V versus SCE. At the potentials $\leq -1.0 \text{ V}$, the films formed were rich in Zn and at the potentials $\geq -0.6 \text{ V}$, an excess of Te was observed. The best stoichiometry of the film was obtained at the deposition potential close to -0.8 V versus SCE. The (111) peak intensities of the XRD patterns of the films deposited at different potentials (not shown) are found to increase with deposition

Table 1. Variation of mercury content in the films for various HgCl₂ concentrations in the bath

| Sl.No | HgCl ₂ concentration in the bath (mM) | Hg content in the film (at %) |
|-------|--|-------------------------------|
| 1 | 0.2 | 12 |
| 2 | 0.4 | 26 |
| 3 | 0.6 | 27 |
| 4 | 0.8 | 28 |
| 5 | 1.0 | 30 |
| 6 | 1.2 | 30 |
| 7 | 1.4 | 30 |

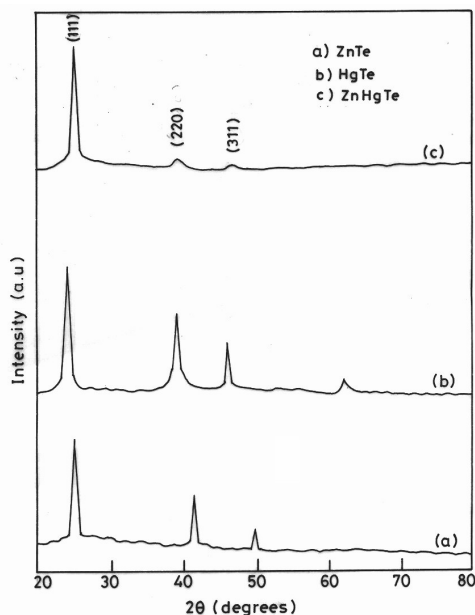


Figure 2. XRD patterns of typical ZnTe, HgTe and ZnHgTe thin films

potentials from -0.6V to -0.9V . At the potentials lesser than -0.9V , the heights of the diffraction peaks were reduced. It indicates that at more negative potentials, films rich in amorphous phase are formed.

3.3. Effect of bath composition

Table 1 shows the HgCl₂ concentration in the solution bath and the corresponding Hg concentration in the deposited film. Increased concentration of HgCl₂ in the deposition bath has resulted in a high Hg content in the films. When the HgCl₂ concentration in the bath is increased beyond 1mM, there was no change of mercury content in the film. Films deposited at increased bath concentration of mercury have shown well-pronounced diffraction peaks of ZnHgTe. At fixed bath composition of mercury, higher mercury content is obtained at more negative potentials. The height of the XRD diffraction peaks increases linearly with TeO₂ concentration. But it reaches a limiting value after 4 mM. The increase of x-ray diffraction peak height at higher TeO₂ concentration can be understood in terms of increase in deposition currents and thus total film thickness. In case of ZnSO₄ concentration, the height of the diffrac-

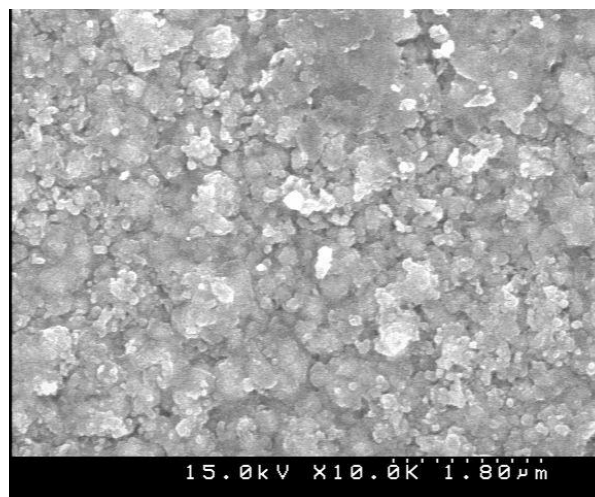


Figure 3. Scanning electron micrograph of as-grown ZnHgTe thin film

tion peaks decreases when the concentration increases from 10 mM to 30mM, and at high ZnSO₄ concentration ($>30\text{mM}$) increased hydrogen evolution was observed, the deposition was found to be irregular and no prominent XRD peaks were obtained. In the present investigation the concentration of precursors were kept as; TeO₂: 4mM, HgCl₂: 1mM and ZnSO₄: 10mM.

3.4. Structural and morphological studies

Figure 2 shows the X-ray diffraction patterns of ZnTe, HgTe and ZnHgTe thin films deposited at potential -0.85V versus SCE at 80°C and at pH of 3.0. Fig.2 (a) shows the XRD pattern of the film deposited with the bath solution of 10 mM ZnSO₄ and 4 mM TeO₂, and it shows the reflection peaks associated with ZnTe. Fig.2 (b) shows the XRD pattern of the film deposited with the bath solution of 1 mM HgCl₂ and 4 mM TeO₂, and these reflections are corresponding to HgTe. Fig. 2(c) shows the film deposited using the electrolyte with all the three precursors. From the XRD patterns of ZnHgTe, it has been observed that the crystallites in the films are preferentially oriented along the (111) face with zinc blende structure. The absence of diffraction peak associated with ZnTe and HgTe in ZnHgTe films indicated that the ZnHgTe films prepared in the present study were of single phase. Hence it is concluded that the crystalline ZnHgTe thin films oriented along the (111) direction can be grown by electrodeposition technique. The inter-planer spacing 'd' for the (111) plane was calculated using the Bragg's relation.

$$d = n\lambda / 2\sin\theta$$

The lattice constant 'a' of the electrodeposited ZnHgTe films of various Hg content was determined by using the relation

$$a = d / \sqrt{(h^2 + k^2 + l^2)}$$

The measured values of lattice constants are in between ZnTe (6.1026 \AA) and HgTe (6.453 \AA). The average grain size (D) of the as-deposited films was determined from the (111) peak using

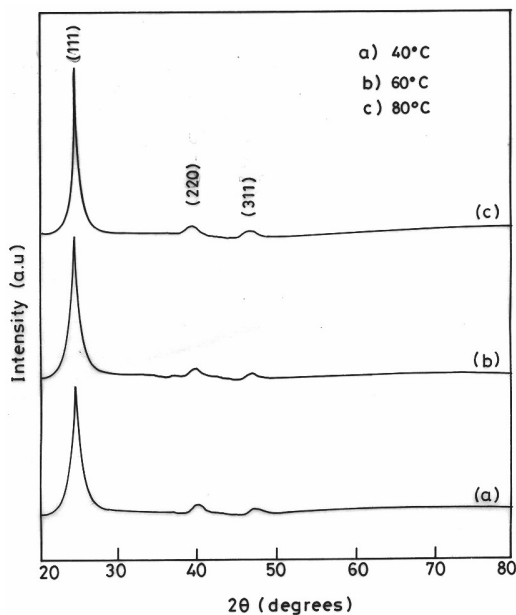


Figure 4. XRD patterns of ZnHgTe films deposited at different bath temperatures (Bath conditions : 4 mM TeO₂, 1 mM HgCl₂, 10 mM ZnSO₄, pH = 3.2)

the Debye-Scherrer formula,

$$D = 0.9\lambda / B \cos \theta_B$$

where λ is the wavelength of x-ray used and B is the full width at half maximum (FWHM) of (111) peak of XRD pattern. The determined grain size of the as-deposited film is about 20 nm.

Figure 3 shows the scanning electron micrograph of as-deposited films. In the optimized condition, the surface of the film is smooth showing grains of different sizes and well covering the substrate. Isolated islands are found, some larger spots are also observed but they are actually the aggregation of the smaller islands.

Effect of bath temperature on structural properties

The XRD patterns of typical ZnHgTe films deposited at different bath temperatures are shown in Figure 4. The bath temperature affects the nature of the films and high temperatures are required to achieve crystalline films. ZnHgTe films deposited at room temperature were found to be amorphous and broad XRD peaks were observed. However, these peaks started to increase above 40°C and the peak positions indicate the presence of HgZnTe. It is found that higher deposition temperature led to the formation of well-crystallized cubic alloy films. Moreover, higher deposition temperature resulted in thicker films with improved crystallinity as revealed by the intense diffraction peaks. HgZnTe films deposited at 80°C were used for further characterization. At temperatures above 80°C, the current densities were found to be higher (>1.5 mA cm⁻²). These high current densities led to the formation of films with rough surface with poor adhesion. The thickness of the film was found to increase linearly with temperature and it is obvious that the temperature affects the rate of release of ions. The (111)

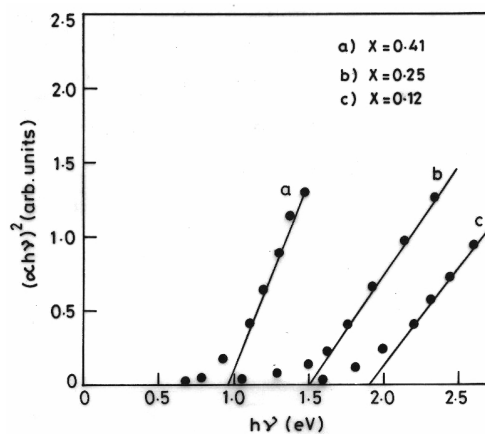


Figure 5. Variation of $(\alpha hv)^2$ versus hv for a typical ZnHgTe thin film

peak of XRD patterns of the films deposited at higher temperature has shown sharper peaks and small FWHM and resulted in the enhancement of crystallite size in the films deposited at higher temperatures.

3.5. Optical studies

The variation of energy gap with composition was determined from the room temperature optical absorption experiments and spectral dependence. The optical data was used to plot a graph of $(\alpha hv)^2$ vs hv , where α is the optical absorption coefficient of the material and hv the photon energy. Figure 5 shows the plot of $(\alpha hv)^2$ vs hv for the films with Hg contents (x value) of 0.12, 0.25 and 0.41. The band gap E_g values have been calculated from the linear fit of the $(\alpha hv)^2$ vs hv plot giving the values 1.9 eV, 1.5 eV and 0.9 eV corresponding to the Hg contents 0.12, 0.25 and 0.41, respectively. This linear dependence showed by α^2 with hv indicates that the transition is direct. The energy gap values obtained for the ZnHgTe films deposited in this work are well within the limits of ZnTe and HgTe. Alloy composition of the films may also be estimated from these optical data.

3.6. Electrical studies

The conductivity type of the electrodeposited Zn_{1-x}Hg_xTe thin film was studied by the hot probe method. The as-deposited films in the optimized condition were found to be p-type. The electrical resistivity of the as-deposited and annealed films was determined by room temperature I-V characteristics studies. I-V characteristics plot showed a linear response in all the films. The resistivities measured from the I-V characteristics plot of as-deposited and annealed films with varying Hg content in Zn_{1-x}Hg_xTe films are found to be in the order of 10⁴ ohm.cm. The resistivity of the as-deposited Zn_{1-x}Hg_xTe film was found to decrease with Hg content in the film. Annealing the deposited films at 200°C in air for 30 minutes reduces the electrical resistivity from 10⁴ to 10³ ohm.cm and this could be attributed to the recrystallization of the as-deposited films, which in turn improves the carrier mobility by diminishing the grain boundaries.

4. CONCLUSIONS

Polycrystalline ZnHgTe thin films were successfully synthesized from acidic solution baths using electrodeposition in the galvanostatic mode. The preparation of stoichiometric films could be achieved by appropriate selection of the growth parameters. The as-grown films presented excellent adherence and relatively good morphological and crystalline properties, as inferred from SEM and XRD analysis. The films exhibited zinc blende structure with predominant (111) orientation. Annealing the films at 200°C resulted in the improvement of crystallinity of the films. Optical absorption studies revealed a direct band gap and a band gap tailoring is observed with the change of Hg content in the films. The electrical resistivity of the films is found to decrease with increase in the Hg content in the films.

5. ACKNOWLEDGEMENT

The authors acknowledge the financial support through the grant G38618U

REFERENCES

- [1] Aried Sher, D. Eger and A. Zemel, *Appl. Phys. Lett.* 46, 59 (1985)
- [2] R. Triboulet, *J. Cryst. Growth.* 86, 79 (1988)
- [3] C. Nguxen Van Huong, R. Triboulet and P. Lemasson, *J. Cryst. Growth.* 101, 311 (1990)
- [4] A. Rasvid, A. Sher and Zussman, *J. Phys. D: Appl. Phys.* 68, 3592 (1990)
- [5] R. Triboulet, A. Lasbley, B. Toulouse and R. Granger, *J. Cryst. Growth* 79, 695 (1986)
- [6] R. Granger, A. Lasbley, S. Rolland, C. M. Pelletier and R. Triboulet, *J. Cryst. Growth.* 86, 682 (1988)
- [7] P. Fajardo, J. Sanz-Maudes, T. Rodriguez, M. A. Gonzalez and R. Triboulet, *J. Cryst. Growth* 101, 872 (1990)
- [8] K. Prabakar, S. Venkatachalam, Y. L. Jeyachandran, SA. K. Narayandas and D. Mangalraj, *Sol. Energy Mater. & Sol. Cells.* 81, 1 (2004)
- [9] N. B. Chaure, Shweta Chaure and R. K. Pandey, *Sol. Energy Mater. & Sol. Cells.* 81, 39 (2004)
- [10] Ariel Sher and Alex Tsigelman, *J. Vac. Sci. Technol.* A8, 1093 (1990)
- [11] R. Granger and C. M. Pelletier, *J. Cryst. Growth.* 117, 203 (1992)
- [12] S. Rolland, R. Granger and R. Triboulet, *J. Cryst. Growth* 117, 208 (1992)